

Correspondence

CT Filtration Aliasing Artifacts

Carl R. Crawford

Abstract—In a continuous implementation of filtered backprojection for computerized tomography (CT), projections are filtered prior to backprojection. The filter has a frequency response that is given by the absolute value of the frequency component. When backprojection is implemented in a discrete environment, the filtration operation can be derived by sampling the filter either in the Fourier or spatial domains. It is shown that the Fourier domain version leads to a dc shift and some low frequency shading in the resulting reconstructions because of aliasing of the filter. The primary purpose of this paper is to show that the aliasing occurs because the inverse Fourier transform of a band-limited version of the continuous filter has infinite spatial extent. A method is also proposed to reduce the aliasing artifacts.

I. INTRODUCTION

The filtered backprojection algorithm allows for the reconstruction of a two-dimensional function from a set of one-dimensional projections [1]. As the name of the algorithm implies, the projections are filtered prior to backprojection. In a continuous implementation of filtered backprojection, the frequency response of the filter is given by the absolute value of the frequency component. In a discrete implementation of filtered backprojection, the filtration step can be derived by sampling in either the Fourier or spatial domains [2]–[4]. The reconstructions that result from these two different filtration methods are virtually identical. However, the method based on Fourier sampling generates a slight object-dependent dc shift and some low-frequency shading artifacts in the resulting reconstructions. In applications where the resulting images are used for quantitative analysis, the shift and the shading will be problematic. The differences in the reconstructions obtained with the two filtration methods have been pointed out in a number of papers [2]–[9]. The primary purpose of this paper is to show that the errors in the Fourier filtration method are due to aliasing. The aliasing occurs because the inverse Fourier transform of a band-limited version of the continuous filter has infinite spatial extent. The underlying mathematics will be reviewed in Section II. In Section III, it will be shown that the dc shift and the shading are due to aliasing. Also in Section III, a method will be shown to reduce the effects of the aliasing.

II. MATHEMATICAL BACKGROUND

In this section, the often used approximations needed to implement the filtered backprojection algorithm in a discrete environment are described. The discussion here focuses on reconstructions from the parallel projection data. The material that is presented is a summary of standard material that is found in the literature [2]–[4]. It is presented here in order to emphasize the origins of the two filtration operations and to develop notation that will be required in the next section.

Consider a two-dimensional function $g(x, y)$. A parallel projec-

tion at angle θ , $P(\theta, t)$, is given by

$$P(\theta, t) = \int_{-\infty}^{\infty} \int_{-\infty}^{\infty} g(x, y) \delta(x \cos \theta + y \sin \theta - t) dx dy. \quad (1)$$

If the projections are known for all θ between zero and π , the original function can be exactly reconstructed by backprojecting filtered versions of the projections [1]. The filtered projections are given by

$$Q(\theta, t) = \int_{-\infty}^{\infty} S(\theta, f) |f| e^{j2\pi ft} df \quad (2)$$

where $S(\theta, f)$ is the Fourier transform of $P(\theta, t)$ given by

$$S(\theta, f) = \int_{-\infty}^{\infty} P(\theta, t) e^{-j2\pi ft} dt \quad (3)$$

and the reconstruction filter is $|f|$. The operation of backprojection for reconstructing $g(x, y)$ is described by

$$g(x, y) = \int_0^{\pi} Q(\theta, x \cos \theta + y \sin \theta) d\theta. \quad (4)$$

Equation (4) presupposes that an infinite number of projections are known for θ from zero to π . Equations (2) and (3) imply that the projections are known at infinitesimal sampling intervals. In order to reduce the amount of information required, a number of approximations and simplifications are made.

Instead of trying to obtain the tomograph for the entire xy -plane, only a disk of radius T is reconstructed. Distortions occur if the object is not zero outside of this region. Most applications have the object to be scanned immersed in air or water. The projection data is normalized to zero for ray paths that include only the air or water [10].

Since the object is zero outside the disk, the projections $P(\theta, t)$ are also zero for $|t| > T$. To obtain the exact image an infinite number of samples are needed over the interval $|t| < T$. If the projections are approximately band-limited $S(\theta, f) \approx 0$ for $|f| > B$ and if more than $4BT$ samples are used practically all the significant information about the projections can be recovered because of the sampling theorem. Let N be the number of samples. The sampled projection $P_s(\theta, i)$ can be found from the projection data as follows:

$$P_s(\theta, i) = P\left(\theta, -T + \frac{T}{2} + i\tau\right), \quad (5)$$

$$i = 0, 1, \dots, N-1, \quad \tau = \frac{2T}{N}.$$

When the projections are assumed to be of finite bandwidth B and finite order (which means that the entire band-limited signal may be represented by a finite number of samples taken at the Nyquist rate), the samples $Q_s(\theta, i)$ of the filtered projections $Q(\theta, t)$ can be obtained from the sampled projections by replacing the Fourier integrals in (2) and (3) with discrete Fourier transforms (DFT)

$$Q_s(\theta, i) = \frac{1}{M} \sum_{k=-M/2}^{M/2-1} S_s(\theta, k) R(k) e^{j2\pi ik/M} \quad (6)$$

Manuscript received January 15, 1990; revised July 7, 1990.
The author is with the Applied Science Laboratory, GE Medical Systems, Milwaukee, WI 53201.
IEEE Log Number 9041387.

and

$$S_s(\theta, k) = \sum_{i=0}^{N-1} P_s(\theta, i) e^{-j2\pi ik/M} \quad (7)$$

where M is the length of the inverse DFT, it has been assumed that M is even, and $R(k)$ is defined as follows:

$$R(k) = \begin{cases} k \frac{2B}{M}, & k = -\frac{M}{2}, \dots, \frac{M}{2} - 1. \end{cases} \quad (8)$$

The method of obtaining the filtered projections using (6) will be denoted the *Fourier* method. The method can be implemented as indicated with (6) and (7). Alternatively, the filtration can be implemented using numerical convolution of the sampled projections and the inverse DFT of $R(k)$. The discrete convolution may be implemented directly on a general purpose computer. However, it is usually much faster to implement (6) and (7) in the frequency domain using fast Fourier transforms (FFT). For the frequency domain implementation it is only possible to perform periodic or circular convolutions and the convolution required is aperiodic. To eliminate the interference artifacts inherent with periodic convolution the projection data have to be padded with sufficient number of zeros. It can be shown that if P_s is padded with zeros so that it is at least $M = (2N - 1)$ elements long, interperiod interference over the N samples of Q_s is avoided [11].

An alternative implementation of the filtration step is obtained by only invoking the assumption of finite bandwidth. Since the projections are bandlimited it does not matter what the filter in (2) is for $|f| > B$. Letting it be zero results in

$$H(f) = \begin{cases} |f|, & |f| \leq B \\ 0, & \text{elsewhere} \end{cases} \quad (9)$$

The function corresponds to the following impulse response in the spatial domain

$$h(t) = \frac{B \sin 2\pi Bt}{\pi t} - \left(\frac{\sin \pi Bt}{\pi t} \right)^2. \quad (10)$$

If the projections and $h(t)$ are sampled at the Nyquist frequency it follows that $\tau = 1/(2B)$. Then it can be shown using (2) that the samples of the filtered projections are given by

$$Q_s(\theta, i) = \tau \sum_{l=-(N-1)}^{N-1} P_s(\theta, i-l) h_s(l), \quad i = 0, \dots, N-1 \quad (11)$$

where (11) follows from the fact that each sampled projection is zero outside the range $(0, N-1)$ for its index. The sampled function $h_s(l)$ is obtained by substituting $t = l\tau$ in (10)

$$h_s(l) = \begin{cases} B^2, & l = 0 \\ 0, & l \text{ even} \\ -\frac{4B^2}{l^2\pi^2}, & l \text{ odd} \end{cases} \quad (12)$$

Equation (11) implies that in order to know $Q_s(\theta, t)$ exactly at the sampling points the length of the sequence $h_s(l)$ used should be from $l = -(N-1)$ to $l = (N-1)$.

The method of obtaining the filtered projections using (11) will be denoted the *Spatial* method. The discrete convolution in (11) may be implemented directly on a general purpose computer or it can be implemented with FFT algorithms. The use of specially designed hardware makes the direct implementation of (11) as fast or faster than the frequency domain implementation.

The continuous filtered projections, in either of the two methods, can be recovered exactly by low-pass filtering. In practice this is too computationally expensive and linear interpolation is used.

The next simplification is the replacement of the integral in (4)

with a summation. This is needed because in any real system there can only be a finite number of projections. If there are K equally spaced projections, using (4), the reconstructed image can be approximated with

$$g(x, y) \approx \frac{\pi}{K} \sum_{i=0}^{K-1} Q'(\theta_i, x \cos \theta_i + y \sin \theta_i), \quad \theta_i = i \frac{\pi}{K} \quad (13)$$

where Q' is a linearly interpolated approximation to Q . Equation (13) is valid for any point (x, y) , but only a finite number of picture points can be reconstructed in a computer implementation. Since the picture is zero outside of a disk of radius T only a square of dimensions $2T$ by $2T$ will be considered. This will be sampled at W^2 points.

III. FILTRATION ALIASING ARTIFACTS

Fig. 1(a) shows the reconstruction along a diameter of a disk of radius 7.5 cm. The Spatial method was used to obtain the filtered projections. The reconstruction along a diameter will be denoted a center line profile. A point source and a point detector were simulated. The disk has density 1000 and the background has a value of zero. The parameters of the reconstruction were $N = K = 64$, $M = 128$, and $W = 128$. The only degradation noticeable in this profile is the smearing of the edges and some ringing. The degradation occurs because the projections of a disk have an infinite bandwidth and the projections are sampled, thus a low-pass filter is introduced. Fig. 1(b) is the center line profile when the Fourier method is used to obtain the filtered projections. The only difference between these two figures appears to be a dc shift in all the values and a slight upward shading. The shading is indicated by the curvature at the center of the profile.

The source of the differences between the Fourier and Spatial methods can be seen by comparing both methods in the Fourier domain. Fig. 2 shows the difference between the DFT of the Spatial method's filter h_s and the filter in the Fourier method, $R(k)$. Only the first few terms are shown because the difference function tends to zero. At dc it is seen that the Spatial method's filter has a positive value because the Fourier method's filter is zero. This is the source of the dc shift in the two reconstructions shown in Fig. 1. The differences at the next few frequency components lead to the shading. The rest of this section deals with the origin of the differences shown in Fig. 2 and methods to correct for them.

The filter used in the Fourier method $R(k)$ is a sampled version of the filter $H(f)$ given in (9). The impulse response corresponding to $H(f)$, given in (10), has an infinite spatial extent. Thus, just as aliasing takes place when a nonband-limited signal is sampled in the space domain causing aliasing in the frequency domain, aliasing will occur in the space domain because of sampling in the frequency domain. The function that corresponds to $R(k)$ in the space domain can be obtained by taking the inverse DFT of (8) which results in

$$r(i) = h_s(i) + a_s(i) \quad (14)$$

where

$$a_s(i) = - \sum_{\substack{k=-\infty \\ k \neq 0}}^{\infty} \left(\frac{B \sin \frac{\pi}{2} (i - kM)}{\frac{\pi}{2} (i - kM)} \right)^2. \quad (15)$$

The function $r(i)$ is defined for all values of the index i and is periodic with period M . According to (11), only the values of $r(i)$ for i in the range $[-(N-1), N-1]$ are required to perform the filtration.

The filtered projection in the Fourier method can be obtained by convolving $P_s(\theta, i)$ with $r(i)$

$$Q(\theta, i) = [h_s(t) * P_s(\theta, i)] + [a_s(i) * P_s(\theta, i)] \quad (16)$$

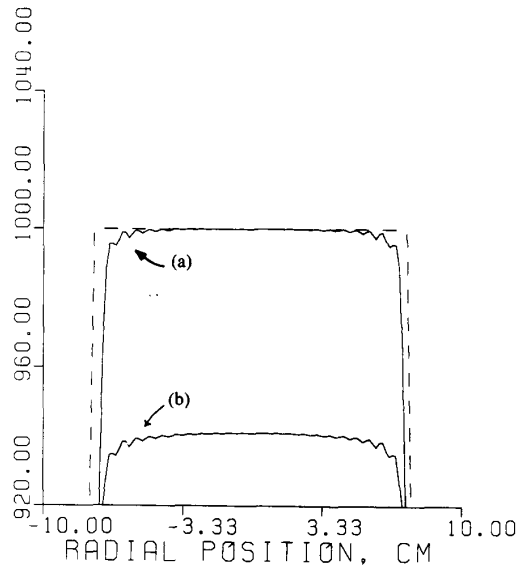


Fig. 1. Center line profiles of the reconstructions of a disk of radius 7.5 cm. Reconstructions were made with (a) the Spatial method and (b) with the Fourier method. The dashed line is the theoretical center line profile. The scale has been expanded in order to emphasize artifacts. Values outside of the scale were set to the limit values of the scale.

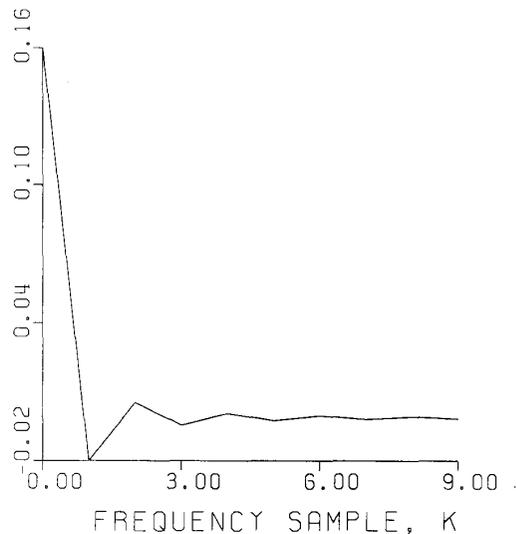


Fig. 2. Difference between the DFT of the Spatial method's filter h_s and the filter used in the Fourier method, $R(k)$.

where the $(*)$ indicates convolution. The first term of (16) reduces to the filtered projection obtained using the Spatial method. The second term must cause the dc shift and the shading. From (15), it is seen that the sequence a_s is negative or zero. The projections of a disk are positive definite. The second convolution in (16) represents the difference between the filtered projections obtained by Fourier and Spatial methods. For the case of a disk, the convolution between a negative and positive sequence is a negative sequence. Adding negative terms in the filtered projection causes at least the negative dc bias in the reconstruction. The bias is object-dependent because the error occurs in the filtration step during filtered backprojection. Another way to verify this observation is to

look at the dc term in $a_s(i)$. The dc term D is given by

$$\begin{aligned} D &= \tau \sum_{i=-M/2}^{M/2-1} a_s(i) = \tau \sum_{i=-M/2}^{M/2-1} [r(i) - h_s(i)] \\ &= -\tau \sum_{i=-M/2}^{M/2-1} h_s(i) \end{aligned} \quad (17)$$

where the second part of the equation follows from (14) and the third part follows from (8). Equation (17) can be evaluated with (12) yielding

$$D = -\frac{2B^2\tau}{\pi^2} \psi' \left(\frac{M-2}{4} \right) \quad (18)$$

where the following equation was utilized in the simplification [12, eq. (5.11.33)]

$$\sum_{k=0}^{n-1} \frac{1}{(2k+1)^2} = \frac{1}{8} \left[\pi^2 - 2\psi' \left(\frac{1}{2} + n \right) \right] \quad (19)$$

$\psi(x)$ is the Psi (or Digamma) function defined by

$$\psi(x) = \frac{\Gamma'(x)}{\Gamma(x)}. \quad (20)$$

The prime as a superscript indicates a derivative. An asymptotic expansion for $\psi'(x)$, when x is large, is given by [13, eq. (6.4.12)]

$$\psi'(x) \approx \frac{1}{x} + \frac{1}{2x^3} + \frac{1}{6x^5} - \dots \quad (21)$$

Therefore, (18) can be approximated with

$$D \approx -\frac{N}{M} \frac{1}{\pi^2} \frac{1}{T}. \quad (22)$$

A modified filter for the Fourier method can be obtained when the value obtained from (22) is subtracted from $R(0)$. The reconstruction that results with the modified filter is shown in Fig. 3(a). It is seen that most of the dc shift has been removed but there still is some shading present. It will now be shown that the remainder of the dc shift and the shading can be eliminated by replacing the first few values of $R(k)$ with the DFT of h_s .

Let $H_s(k)$ be the DFT of the filter for the Spatial method

$$H_s(k) = \sum_{i=(-M/2)}^{(M/2)-1} h_s(i) e^{-j2\pi ik/M}, \quad k = \frac{-M}{2}, \dots, \frac{M}{2} - 1. \quad (23)$$

If (12) is substituted in (23), and (19) and (21) are used, the following is obtained:

$$H_s(k) \approx B^2(1 - S_M(k)) + \frac{8B^2}{\pi^2 M} S_M(k) \quad (24)$$

where

$$S_M(k) = \frac{\sum_{i=0}^{(M/4)-1} \frac{\cos 2\pi k(2i+1)/M}{(2i+1)^2}}{\sum_{i=0}^{(M/4)-1} (2i+1)^{-2}}. \quad (25)$$

A closed-form solution of (25) could not be determined. Table I shows the values of $S_M(k)$ for typical values of M and k that were obtained by direct evaluation of (25). Fig. 3(b) shows the center line profile of the disk after the values of $R(k)$, for $k = 1, 2$, are replaced with the values obtained with (24) (after multiplication with τ). Comparing this reconstruction to Fig. 1(a) shows that the Fourier method with the dc and two lowest frequency terms corrected will yield approximately the same results as obtained with the Spatial method.

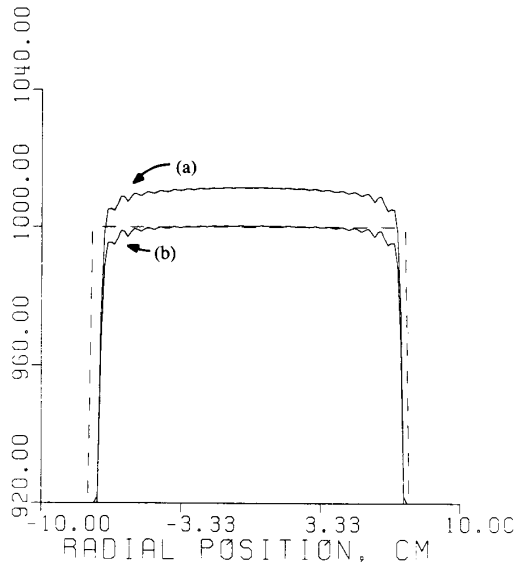


Fig. 3. Center line profiles of the reconstruction of the disk with filtration done with modified versions of the Fourier method: (a) is with compensation for dc errors and (b) is with correction for dc and the first two frequency components.

TABLE I
TYPICAL VALUES OF THE FUNCTION $S_M(k)$

M	$k = 1$	$k = 2$	$k = 3$
32	0.90071034	0.76843792	0.64170682
64	0.95101577	0.88569993	0.82317317
128	0.97566682	0.94321388	0.91215277
256	0.98787266	0.97169709	0.95621610
512	0.99394625	0.98587108	0.97814298
1024	0.99697590	0.99294168	0.98908007
2048	0.99848813	0.99647111	0.99454314

The Fourier domain filter is also known as the Ramachandran-Lakshminarayanan kernel [14]. In order to improve the signal-to-noise ratio in reconstructions, the projections can be low-pass filtered [15]. Usually, the filtration required by the reconstruction algorithm and the low-pass filtering is performed in one step by filtering the projections with the convolution of the low-pass filter and the reconstruction kernel. If the low-pass filter is sampled in the Fourier domain, then aliasing will occur because the filter has infinite spatial extent. The Shepp-Logan kernel is a commonly used combination of the reconstruction kernel and a low-pass filter [16]. Because the Shepp-Logan kernel is derived from a sampled version of the inverse continuous Fourier transform, aliasing will not occur for the low-pass component.

The effects of aliasing can be reduced by zero-padding the projections before taking the initial DFT when the projections are filtered in the Fourier domain. The reduction in aliasing artifacts is confirmed by the presence of the length of the DFT, M , in the denominator of (22). The use of zero-padding, however, can significantly increase the time required to perform the filtration step.

IV. CONCLUSION

Two methods for filtering projections for the filtered backprojection reconstruction algorithm have been evaluated. The two meth-

ods were based on derivations made in the spatial and Fourier domains and therefore they are denoted the Spatial and Fourier methods, respectively. Both methods can be applied in either the spatial or Fourier domains. The Fourier method of filtration produces images with dc shifts and low-frequency shading. The Spatial method of filtration does not generate similar artifacts. It has been shown that the artifacts result because of aliasing artifacts that arise when a spatial waveform with infinite extent is sampled in the Fourier domain. It was also shown that it is possible to correct the artifacts generated with the Fourier method by replacing the dc and the first two frequency components with the corresponding terms from the discrete Fourier transforms of the filter used in the Spatial method.

ACKNOWLEDGMENT

The author would like to thank A. Kak for stimulating the interest that led to this work. The comments of G. Gullberg, K. King, A. Lonn, and M. Slaney are greatly appreciated. D. Birzer and D. Stenske helped prepare the manuscript.

REFERENCES

- [1] R. N. Bracewell and A. C. Riddle, "Inversion of fan-beams scans in radio astronomy," *Astrophys. J.*, vol. 150, pp. 427-434, 1967.
- [2] C. R. Crawford and A. C. Kak, "Aliasing artifacts in computerized tomography," *Appl. Opt.*, vol. 18, pp. 3704-3711, 1979.
- [3] A. C. Kak and M. Slaney, *Principles of Computerized Tomographic Imaging*. New York: IEEE Press, 1988.
- [4] A. C. Kak, "Computerized tomography with X-ray, emission, and ultrasound sources," *Proc. IEEE*, vol. 67, pp. 1245-1272, 1979.
- [5] A. Rosenfeld and A. C. Kak, *Digital Picture Processing*. New York: Academic, 1982.
- [6] S. J. Glick, M. A. King, and B. C. Penney, "Characterization of the modulation transfer function of discrete filtered backprojection," *IEEE Trans. Med. Imaging*, vol. 8, pp. 203-213, 1989.
- [7] S. H. Manglos, R. J. Jaszczak, C. E. Floyd, L. J. Hahn, K. L. Greer, and R. E. Coleman, "A quantitative comparison of attenuation-weighted backprojection with multiplicative and iterative postprocessing attenuation compensation in SPECT," *IEEE Trans. Med. Imaging*, vol. 7, pp. 127-134, 1988.
- [8] G. T. Gullberg, H. B. Hu, and B. M. W. Tsui, "A convolution algorithm that compensates for uniform attenuation in SPECT imaging," *J. Nucl. Med.*, vol. 28, p. 506, 1987.
- [9] S. W. Rowland, "Computer implementation of image reconstruction formulas," in *Image Reconstruction from Projections: Implementation and Applications*, G. T. Herman, Ed. New York: Springer-Verlag, 1979.
- [10] A. C. Kak, C. V. Jakowatz, N. Baily, and R. Keller, "Computerized tomography using video recorded fluoroscopic imaging," *IEEE Trans. Biomed. Eng.*, vol. BME-24, pp. 157-169, 1977.
- [11] C. V. Jakowatz and A. C. Kak, "Computerized tomography using X-rays and ultrasound," *Purdue Univ. Res. Rep. TR-EE 76-26*, 1976.
- [12] E. R. Hansen, *A Table of Series and Products*. New York: Prentice-Hall, 1975.
- [13] M. Abramowitz and I. A. Stegun, *Handbook of Mathematical Functions*, AMS 55. Washington, DC: National Bureau of Standards, 1968.
- [14] G. N. Ramachandran and A. V. Lakshminarayanan, "Three-dimensional reconstruction from radiographs and electron micrographs: Application of convolution instead of Fourier Transforms," in *Proc. Nat. Acad. Sci.*, vol. 68, 1971, pp. 2236-2240.
- [15] S. M. Blumenfeld and G. H. Glover, "Spatial resolution in computed tomography," in *Radiology of the Skull and Brain—Technical Reports of Computed Tomography*, T. H. Newton and D. G. Potts, Ed. London, England: C. V. Mosby Co., 1981.
- [16] L. A. Shepp and B. F. Logan, "The Fourier reconstruction of a head section," *IEEE Trans. Nucl. Sci.*, vol. NS-21, pp. 21-43, 1974.